

Molecular characterization of the recombinant iron-containing alcohol dehydrogenase from the hyperthermophilic Archaeon, *Thermococcus* strain ES1

Xiangxian Ying · Amy M. Grunden ·
Lin Nie · Michael W. W. Adams · Kesen Ma

Received: 16 October 2008 / Accepted: 27 November 2008 / Published online: 25 December 2008
© Springer 2008

Abstract The gene encoding a thermostable iron-containing alcohol dehydrogenase from *Thermococcus* Strain ES1 (ES1 ADH) was cloned, sequenced and expressed in *Escherichia coli*. The recombinant and native ES1 ADHs were purified using multistep column chromatography under anaerobic conditions. Both enzymes appeared to be homotetramers with a subunit size of 45 ± 1 kDa as revealed by SDS-PAGE, which was close to the calculated value (44.8 kDa). The recombinant ADH contained 1.0 ± 0.1 g-atom iron per subunit. Both enzymes were sensitive to oxygen with a half-life upon exposure to air of about 4 min. The recombinant enzyme exhibited a specific activity of 105 ± 2 U mg⁻¹, which was very similar to that of the native enzyme (110 ± 3 U mg⁻¹). The optimal pH-values for both enzymes for ethanol oxidation and acetaldehyde reduction were 10.4 and 7.0, respectively. Both enzymes also showed similar temperature-dependent

activities, and catalyzed the oxidation of primary alcohols, but there was no activity towards methanol and secondary alcohols. Kinetic parameters of the enzymes showed lower K_m -values for acetaldehyde and NADPH and higher K_m -values for ethanol and NADP⁺. It is concluded that the gene encoding ES1 ADH was expressed successfully in *E. coli*. This is the first report of a fully active recombinant version of an iron-containing ADH from a hyperthermophile.

Keywords Iron-containing alcohol dehydrogenase · Heterologous expression · Hyperthermophile · Archaea · *Thermococcus*

Introduction

Alcohol dehydrogenases (ADHs) are a group of oxidoreductases that catalyze the interconversion of alcohols and the corresponding aldehyde or ketone. ADHs are ubiquitous and most are dependent on NAD⁺ and/or NADP⁺, and many of them catalyze the synthesis of chiral compounds for use in the pharmaceutical industry (Hummel 1999). NAD(P)⁺-dependent ADHs differ in size and metal content. The metal-free and zinc-containing ADHs have a size of ~250 and ~350 amino acids, respectively, while a typical iron-containing ADH has a larger size varying from 382 to 891 amino acids (Reid and Fewson 1994). It is known that iron-containing ADHs in mesophiles are key enzymes that catalyze the formation of various alcohols such as ethanol, 1,2-propanediol, 1,3-propanediol and 1-butanol (Conway and Ingram 1989; Walter et al. 1992; Zheng et al. 2004; Montella et al. 2005). Thermostable versions of these enzymes are potentially new types of biocatalysts with a range of biotechnological applications

Communicated by H. Santos.

X. Ying · L. Nie · K. Ma (✉)
Department of Biology, University of Waterloo,
200 University Ave. W, Waterloo,
ON N2L 3G1, Canada
e-mail: kma@uwaterloo.ca

A. M. Grunden
Department of Microbiology,
North Carolina State University, Raleigh, NC 27606, USA

M. W. W. Adams
Department of Biochemistry and Molecular Biology,
University of Georgia, Athens, GA 30602, USA

Present Address:
X. Ying
Zhejiang University of Technology,
310014 Zhejiang, China

(Li and Stevenson 1997; Antoine et al. 1999; Ma and Adams 1999; Ma and Adams 2001; Ying et al. 2007). However, only a few iron-containing ADHs have been characterized from the so-called hyperthermophiles, which are defined as organisms that grow optimally at 80°C and above (Stetter 1988).

There are four thermostable iron-containing ADHs available from hyperthermophiles, all from members of the genus *Thermococcus*, and these are *T. litoralis* (Ma et al. 1994), *Thermococcus* strain ES1 (Ma et al. 1995), *T. zilligii* (Li and Stevenson 1997; Ronimus et al. 1997), and *T. hydrothermalis* (Antoine et al. 1999). Recombinant forms of such enzymes are obviously essential for any biotechnological application, and they would also be extremely useful for further characterization studies, such as determining three-dimensional structures and structure/function studies using mutagenesis. Although several genes encoding metal-free and Zn-containing ADHs from hyperthermophiles have been successfully expressed in *Escherichia coli* to yield recombinant forms (Cannio et al. 1996; van der Oost et al. 2001; Hirakawa et al. 2004; Kube et al. 2006; Machielsen et al. 2006), the expression of genes encoding iron-containing ADHs from hyperthermophiles has remained a challenge. Heterologous expression of the gene encoding the iron-containing ADH from *T. hydrothermalis* in *E. coli* is the only example of an iron-containing ADH from a hyperthermophilic archaeon, in which both the recombinant and native ADHs were shown to possess similar general characteristics. However, the native and recombinant *T. hydrothermalis* ADH enzymes were shown to have clear differences in catalytic activity and thermostability (Antoine et al. 1999).

The archaeon *Thermococcus* strain ES1 is an anaerobic heterotroph that grows optimally at 82°C (Pledger and Baross 1989). It has the most thermostable iron-containing ADH of any yet characterized, and the enzyme shows much higher activity in vivo when cells are grown under S⁰-limited growth conditions (Ma et al. 1995). We report here that the gene encoding the iron-containing ADH from *Thermococcus* Strain ES1 has been cloned, sequenced and expressed in *E. coli*. Molecular characterization and comparison of the recombinant and native ADHs showed that they have indistinguishable characteristics, providing the first example of a recombinant hyperthermophilic iron-containing ADH that is fully active.

Materials and methods

Organisms and chemicals

Thermococcus strain ES1 was grown as described previously (Ma et al. 1995). *E. coli* strains XL1-blue and BL21

(DE3) were used for cloning and overexpression of the gene encoding the ES1 ADH, respectively. The *E. coli* strains were grown in Luria Bertani media (LB). Ampicillin (100 µg/ml) was added as needed for plasmid maintenance.

High-grade chemicals and enzymes (lysozyme and DNase I) were commercially available from Sigma-Aldrich (Oakville, ON, Canada). All materials and columns for fast protein liquid chromatography (FPLC) were obtained from Amersham GE Health (Oakville, ON, Canada).

Cloning, sequencing and expression of the gene encoding *Thermococcus* Strain ES1 ADH

All standard molecular biology techniques were performed essentially as described previously (Sambrook and Russell 2001). The *Thermococcus* strain ES1 ADH gene was initially identified by screening an ES1 DNA library. This DNA library was generated by digesting ES1 genomic DNA with the restriction enzyme *EcoRI* and isolating DNA fragments that ranged in size from 2–4 kbp. The restricted DNA was ligated into the pCR-Script plasmid (Stratagene) that had been cut with *EcoRI*. The ligated plasmids were then transformed into competent XL1-Blue MRF' cells (Stratagene). Three hundred transformed colonies were isolated and screened via southern hybridization using a 650 bp biotin-labeled Adh gene probe (Leary et al. 1983) following the Stratagene Illuminator Chemiluminescent Detection system protocol. A plasmid containing a ~3 kbp DNA insert was shown to hybridize to the *adh* probe. The DNA insert was subsequently sequenced and shown to contain the entire ES1 *adh* gene.

The recombinant form of *Thermococcus* strain ES1 ADH was obtained by PCR amplification of the gene encoding the enzyme and its subsequent cloning into the T7-polymerase-driven expression vector pET-21b (Novagen, Milwaukee, WI, USA). For amplification of the ADH gene, the following primers were used: Forward ADH primer 5'-GGGTTCCATATGCTGTGGGAATCCCAGATACCGAT-3' (spanning -9 to +24 on the coding strand) and Reverse ADH primer 5'-GAAGGATCCCTTACGTCACTTGCTAAG-3' (corresponding to +1,210 to +1,236 on the non-coding strand) (MWG Biotech, Huntsville, AL, USA). The sequences in bold print mark recognition sites for the restriction enzymes *NdeI* and *BamHI*, respectively. Amplification was performed using *P. furiosus* DNA polymerase (Stratagene) and a Robocycler 40 thermocycler (Stratagene) with the following parameters: one cycle of denaturation at 95°C for 5 min, annealing at 45°C for 2 min, and extension at 72°C for 1.5 min. This was followed by 39 cycles with a 1 min denaturation at 95°C, 1 min annealing at 52°C, and 1.5 min extension at 72°C. The amplified 1.2 kb ADH gene was gel-purified and

isolated using the Gene Clean III kit (Qbiogene Carlsbad, CA, USA). The ADH gene was subcloned into the blunt end *EcoRV* site of plasmid pCR-Script (Stratagene) to yield plasmid pES1-ADH. The gene was then excised from plasmid pES1-ADH by restriction digest with the enzymes *NdeI* and *BamHI* (Stratagene) and cloned into the *NdeI* and *BamHI* sites in the expression plasmid pET-21b, resulting in plasmid pET-ES1ADH.

Prior to recombinant ADH expression, the gene sequence of ADH in the pET-ES1ADH construct was determined in its entirety by the Molecular Genetics Instrumentation Facility (MGIF) of the University of Georgia. DNA sequences were analyzed using the computer software package MacVector (Accelrys, Burlington, MA, USA).

For expression of the recombinant ADH gene in *E. coli*, plasmid pET-ES1ADH was transformed into strain BL21(λ DE3), which has isopropyl- β -D-thiogalactopyranoside (IPTG) induced expression of T7 RNA polymerase. The recombinant strain was grown in a 100 L fermentor at 37°C using Luria Bertani (LB) as the growth medium supplemented with ampicillin (100 μ g/ml) (University of Georgia BioXpress fermentation facility, Department of Biochemistry). Expression of the plasmid-borne ADH gene was induced by the addition of IPTG (0.4 mM) once the culture had reached an OD₆₀₀ of 0.8. The induced culture was incubated at 37°C for 4 h prior to harvesting the cells.

Purification of the native and recombinant *Thermococcus* strain ES1 ADHs

All purification steps were carried out anaerobically. For purifying the native ADH, frozen cells of *Thermococcus* strain ES1 (15 g, wet weight) were thawed anaerobically in 75 ml buffer A [50 mM Tris buffer containing 5% (v/v) glycerol, 2 mM dithiothreitol (DTT), 2 mM sodium dithionite (SDT) and 0.01 mg mL⁻¹ DNase I, pH 7.8]. The cell suspension was incubated with stirring for 2 h at 37°C. After centrifugation at 10,000 \times *g* for 30 min, the supernatant was collected as the cell-free extract, which was loaded onto a DEAE-Sepharose column (5 \times 10 cm) that had been equilibrated with buffer A. A linear gradient (0–0.35 M NaCl in buffer A) was applied at a flow rate of 3 ml min⁻¹ and the ADH was eluted when a concentration of 0.22 M NaCl in buffer A was reached. The fractions containing ADH activity were pooled and loaded onto a pre-equilibrated hydroxyapatite column (2.6 \times 15 cm) at a flow rate of 1.5 ml min⁻¹. A linear gradient (0–0.5 M potassium phosphate in buffer A) was run and the ADH activity was eluted when the salt concentration was as high as 0.5 M potassium phosphate in buffer A. The fractions containing ADH activity were desalted and concentrated using ultrafiltration with an YM-10 membrane. The concentrated sample was loaded onto a gel filtration column

(2.5 \times 60 cm) pre-equilibrated with buffer A containing 150 mM potassium chloride. The purified native ADH was stored in liquid nitrogen until use.

For purifying the recombinant ADH, frozen *E. coli* cells (10 g) were thawed anaerobically and suspended in 50 ml buffer A. The cell suspension was incubated with stirring for 2 h at 37°C. The resultant *E. coli* cell-extract was incubated for 1 h at 60°C. The denatured proteins and cell debris in the gel-like suspension were removed by centrifugation at 10,000 \times *g* for 30 min. The supernatant was collected and loaded onto a pre-equilibrated DEAE-Sepharose column (5 \times 10 cm) with buffer A. A linear gradient (0–0.35 M NaCl in buffer A) was applied at a flow rate of 3 ml min⁻¹ and the ADH was eluted at a concentration of 0.25 M NaCl in buffer A. The recombinant ADH was judged to be pure by using SDS-PAGE and was stored in liquid nitrogen until use.

Determination of molecular mass

The molecular mass of the enzyme subunit was determined using SDS-PAGE (Laemmli 1970) together with a low molecular mass standard kit (14–97 kDa, Bio-Rad Laboratories, ON, Canada). The native molecular mass of the purified enzyme was estimated using the gel filtration column Superdex 200 (2.6 \times 60 cm). The column was equilibrated with buffer A containing 100 mM KCl at a flow rate of 2 ml min⁻¹ before applying standard protein samples (Pharmacia, NJ, USA) that were blue dextran (molecular mass, Da, 2,000,000), thyroglobulin (669,000), ferritin (440,000), catalase (232,000), aldolase (158,000), bovine serum albumin (67,000), ovalbumin (43,000), chymotrypsinogen A (25,000) and ribonuclease A (13,700). In addition, the size of both native and recombinant ES1ADHs was also determined using mass spectrometry. The enzyme (native or recombinant ES1ADH) was dissolved in 18.2 M Ω cm deionized water and was analyzed via positive electrospray ionization-mass spectrometry (Mass Spectrometry Facility, University of Waterloo, Waterloo, ON, Canada).

Enzyme assay and protein determination

Alcohol dehydrogenase activities were determined anaerobically at 80°C by measuring the ethanol-dependent reduction of NADP⁺ or the acetaldehyde-dependent oxidation of NADPH at 340 nm. Unless specifically stated, the enzyme assay was carried out in duplicate using the standard reaction mixture for ethanol oxidation, which contained 100 mM CAPS (pH 10.4), 90 mM ethanol, and 0.4 mM NADP⁺. The reaction mixture for acetaldehyde reduction was composed of 100 mM HEPES buffer (pH 7.0), 0.4 mM NADPH and 90 mM acetaldehyde. The reaction was initiated by adding 1.5 μ g enzyme. One unit

Fig. 1 Sequence alignment of ESIADH and related iron-containing ADHs. The sequences were aligned using Clustal W (Thompson et al. 1994). Thyr, *T. hydrothermalis*; Tzill, *T. zilligii*; EcoliADH, L-1,2-propanediol dehydrogenase in *E. coli*. TM0820 and TM0920 are putative iron-containing ADHs in *T. maritima*. The typical coenzyme

 Springer

of ADH activity is defined as the formation or oxidation of 1 μ mol of NADPH per min. The protein concentration was determined using the Bradford method and bovine serum albumin served as the standard protein (Bradford 1976).

Characterization of catalytic properties

The optimal pH of ethanol-dependent oxidation of native and recombinant ES1ADHs was determined at 80°C using a set of 100 mM buffers: 4-(2-hydroxyethyl)-1-piperazineethanesulfonic acid (HEPES; pH 6.5, 7.0, 7.5 and 8.0), *N*-(2-hydroxyethyl)-piperazine-*N'*-(3-propanesulfonic acid) (EPPS; pH 8.0, 8.5, 8.8, 9.0), glycine (pH 9.0, 9.5, 10.0) and 3-(cyclohexylamino)-1-propanesulfonic acid (CAPS; pH 10.0, 10.5, 11.0). The optimal pH of acetaldehyde-dependent reduction of native and recombinant ES1ADH was determined using the following buffers (100 mM): citrate (pH 5.5 and 6.0), 1, 4-piperazine-bis-(ethanesulfonic acid) (PIPES; pH 6.0, 6.5 and 7.0), HEPES (pH 7.0, 7.5 and 8.0), EPPS (pH 8.0, 8.5, and 9.0), glycine (pH 9.0 and 9.5). Thermostability of the purified enzymes was tested in a sealed serum bottle at the desired temperature and residual activities at different time intervals were measured. The effect of oxygen on enzyme activity was investigated by vortexing the enzyme sample in the air at room temperature and determining the residual activity at different time intervals after exposure to oxygen. For the test of substrate specificity, various primary and secondary alcohols replaced ethanol in the standard assay mixture.

For obtaining kinetics parameters, various substrate concentrations (0 to $\geq 10 \times$ apparent K_m unless specified) were used for determining the corresponding activities at 80°C when concentrations of the corresponding co-substrates were kept constant and higher than $10 \times$ apparent K_m . Substrates used were NADPH (0, 0.025, 0.05, 0.1, 0.15, 0.2 and 0.4 mM), acetaldehyde (0, 2.3, 4.6, 9.1, 22.3, 27.3, 36.4, 45.5 and 91 mM), NADP⁺ (0, 0.02, 0.04, 0.08, 0.10, 0.15, 0.2, 0.3 and 0.4 mM), and ethanol (0, 4.4, 8.7, 13.0, 17.4, 34.8, 52.2, 70, 87 and 174 mM). Apparent values of K_m and V_{max} were calculated by fitting the data into Michaelis–Menten equation using the SigmaPlot (Systat Software Inc., San Jose, CA, USA). All the reactions followed Michaelis–Menten-type kinetics.

Metal analyses

The metal contents of the purified enzymes were determined using inductively coupled plasma mass spectrometry (VG Elemental PlasmQuad 3 ICP-MS at the Chemical Analysis Laboratory, University of Georgia, USA). The enzyme sample was pretreated to wash off non-binding metals using YM-10 Amicon centrifuge tubes (Millipore, Billerica, MA, USA) in an anaerobic chamber

where the oxygen level was kept below 1 ppm. Ten millimole Tris/HCl (pH 7.8) containing 2 mM DTT was used as washing buffer for the cycles of centrifugation (seven times repeat of filtration and refilling with the washing buffer), and the passthrough was collected as controls for the metal analysis.

Sequence analyses

The homologues of the deduced amino acid sequence of ES1ADH were identified using the BLAST program with the default parameters (Altschul et al. 1997). Additional sequences were retrieved from the Pfam database (Bateman et al. 2002). Sequence alignments and similarity comparisons were initially conducted by the ClustalW method with default parameters (Thompson et al. 1994) and the final alignment was manually performed with the multiple sequence editor MegAlign (DNASTar, Madison, WI, USA). Phylogenetic and molecular evolutionary analyses were constructed using MEGA version 4 (Tamura et al. 2007). Amino acid composition, theoretical isoelectric point and molecular weight were calculated using the ProtParam program at the ExPASy Proteomics Server with standard parameters (Gasteiger et al. 2005). A 3-D structure of ES1ADH monomer was modeled using the Swiss Model server (Peitsch 1995; Guex and Peitsch 1997; Schwede et al. 2003; Kopp and Schwede 2004). PyMOL was used to analyze and visualize the 3-D structure (Delano 2002).

Sequence accession number

The sequence for *Thermococcus* strain ES1 ADH is available in the GenBank database under the accession number EU919177.

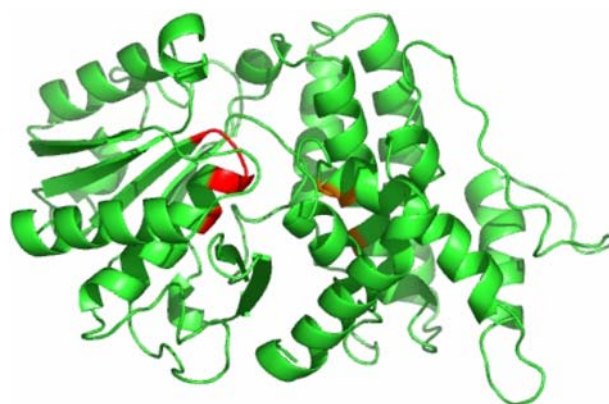


Fig. 2 Predicted tertiary structure of ES1ADH monomer. The 3D structural modeling was run on the Swiss Model server using an iron-containing ADH from *T. maritima* (TM0820; PDB number: 1v1jB) as the template. The structure figure was constructed using PyMOL (Delano 2002). Residues in red, the putative NADP⁺-binding site; residues in orange, the putative iron-binding site

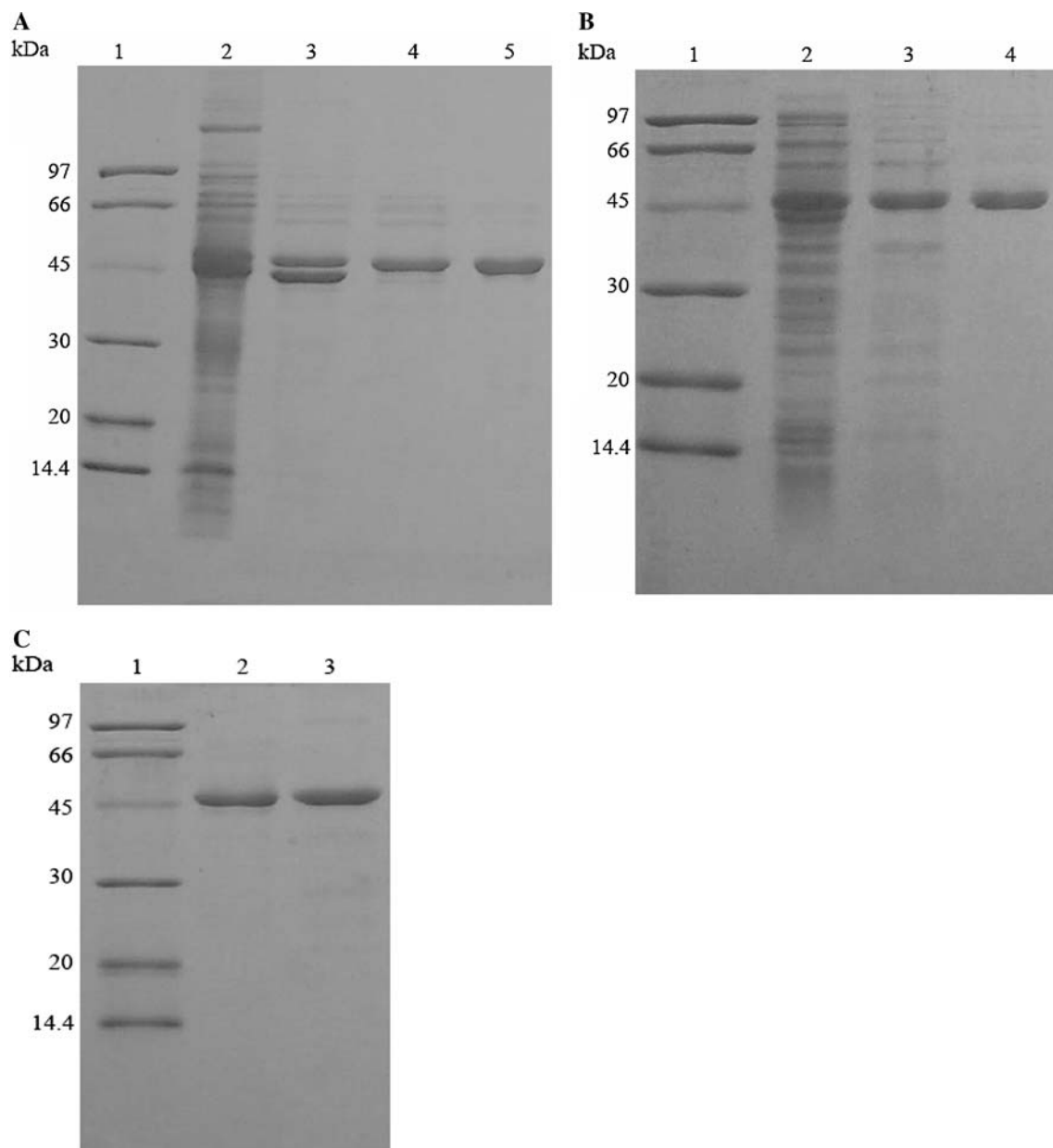


Fig. 3 Analyses of the ADH from *Thermococcus* Strain ES1 (**a**) and the recombinant ES1ADH from *E.coli* (**b**) and the comparison of both purified enzymes (**c**) using SDS-PAGE (12.5%). **a** Lane 1 molecular markers, lane 2 cell-free extract, lane 3 DEAE-Sepharose, lane 4 hydroxyapatite, lane 5 gel filtration. In lanes 2–5 2 µg of protein was

loaded per lane. **b** Lane 1 molecular markers, lane 2 cell-crude extract, lane 3 heat precipitation, lane 4 DEAE-sepharose. In lanes 2–4, 2 µg of protein was loaded per lane. **c** Lane 1 molecular markers, lane 2 1.5 µg native ES1ADH, lane 3 1.5 µg recombinant ES1ADH

Results

Sequence analysis and molecular characterization

The gene encoding *Thermococcus* strain ES1 ADH was identified using labeled DNA to probe plasmid constructs from a *Thermococcus* ES1 DNA library. The ES1 ADH probe had been amplified from ES1 genomic DNA using degenerate primers based on two internal amino acid sequences (ELYKLQFSPR, amino acids 134–143) and

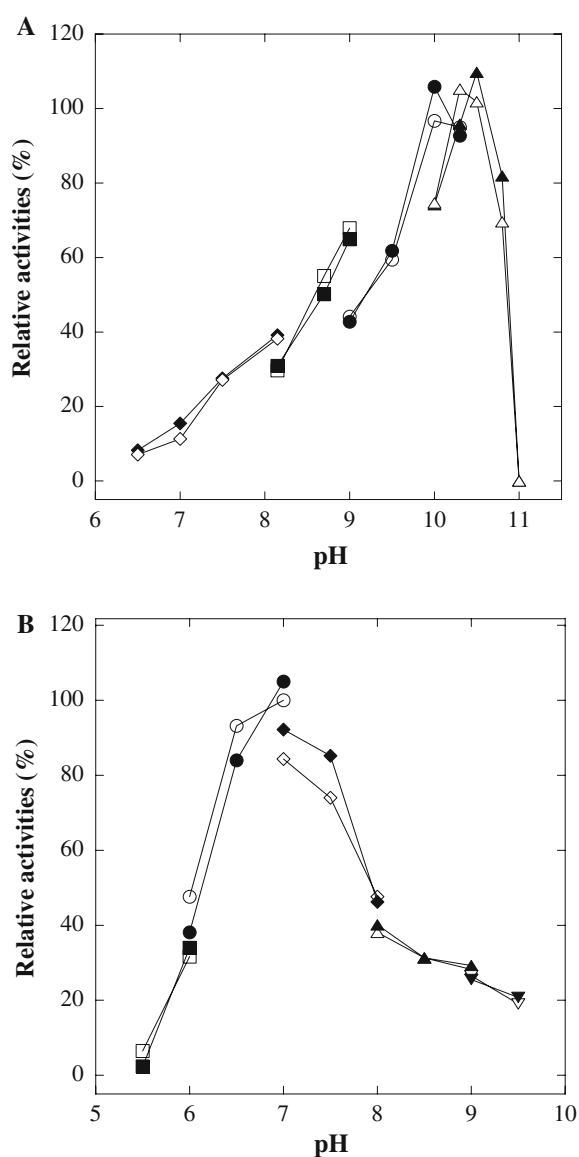
(ILAEIYRPLVPEV, amino acids 315–327) derived from the enzyme purified from native ES1 biomass. The library screen identified a plasmid containing a ~3 kb insert that hybridized to the ADH probe. Sequencing of this plasmid revealed that the *Thermococcus* strain ES1 ADH gene is 1,218 bp in size and encodes a 406 amino acid polypeptide with a calculated isoelectric point (pI) and molecular mass of pH 5.5 and 44.8 kDa, respectively.

BLASTP searches of the nonredundant database with the ES1 ADH amino acid sequence revealed more than 100

Table 1 Purification of the native ADH from *Thermococcus* strain ES1 and the recombinant ES1ADH from *E. coli*

Purification steps	Total protein (mg)	Total activity (U)	Specific activity (U mg ⁻¹) ^a	Purification fold	Yield (%)
Native ES1 ADH					
Cell-free extract	154	862	5.6	1	100
DEAE-sepharose	33.7	797	23.6	4.2	92
Hydroxyapatite	12.9	616	47.8	8.5	71
Gel-filtration	6.1	348	57	10.1	40
Recombinant ES1 ADH					
Cell-crude extract	650	4,445	6.8	1	100
Heat precipitation	145	3,596	24.8	3.6	81
DEAE-sepharose	63	3,326	52.8	7.8	75

^a Enzyme activity was measured in 100 mM EPPS buffer (pH 8.8)



hits; all of them were members of the ADH family, including iron-containing ADH, 1, 3-propanediol dehydrogenase, and alcohol dehydrogenase IV (Altschul et al. 1997). The two best scores were obtained with ADHs from *T. zilligii* and *T. hydrothermalis* (~80% identity). DNA sequence comparison between the ES1, *T. zilligii* and *T. hydrothermalis* ADH coding regions as well as upstream (182 bases) and downstream (124 bases for *T. zilligii* and 382 bases for *T. hydrothermalis*) sequence indicated that all three ADH coding sequences shared 75% identity, whereas there was less than 43% identity amongst the upstream or downstream sequences, indicating that while the ADH gene is highly conserved, sequence surrounding the ADH gene is not well conserved among the three *Thermococci*.

ES1 ADH also showed high degrees of identity (62–72%) to iron-containing ADHs from various thermophilic bacteria such as *Thermoanaerobacter* species, but low degrees of identity (30–32%) to well-characterized ADHs such as those from *E. coli* and *Klebsiella pneumoniae* (Zheng et al. 2004). In particular, ES1 ADH had extremely low sequence identity (<30%) to the iron-containing ADHs from *Thermotoga maritima*. In contrast, the ADH from *Thermotoga hypogea* had 75% sequence identity to TM0820, an iron-containing ADH in *T. maritima* (Ying 2007).

Fig. 4 pH dependency of ES1ADHs for ethanol oxidation (a) and acetaldehyde reduction (b). **a** Open symbols represent the ADH from *Thermococcus* strain ES1 and filled symbols represent the recombinant ADH expressed in *E. coli*. The buffers used were HEPES (diamonds), EPPS (squares), glycine (circles) and CAPS (triangles). The relative activity of 100% is equal to 105.2 U mg⁻¹ of ethanol oxidation activity. **b** Open symbols represent the native ES1ADH. Filled symbols represent the recombinant ES1ADH. The buffers used were sodium citrate (squares), PIPES (circles), HEPES (diamonds), EPPS (vertical triangles), glycine (inverted triangles). The relative activity of 100% corresponds to 28.0 U mg⁻¹ of acetaldehyde reduction activity

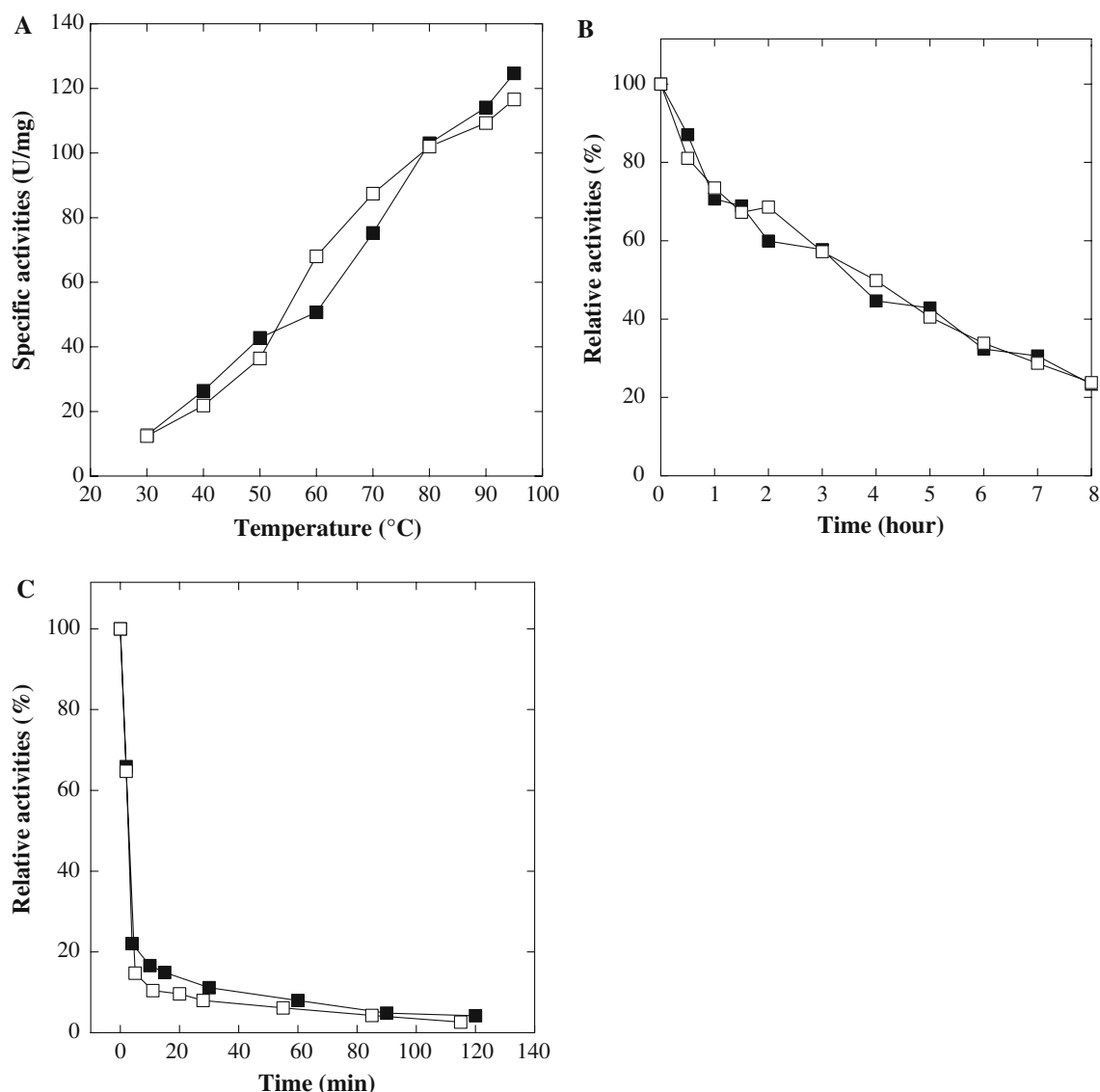


Fig. 5 Temperature-dependent activities (**a**), thermostability (**b**) and oxygen sensitivity (**c**) of both native and recombinant ES1 ADHs. **a** Filled squares native ES1ADH, open squares recombinant ES1ADH. **b** Filled squares native ES1ADH, open squares recombinant

ES1ADH, incubated at 95°C. **c** Filled squares native ES1ADH, open squares recombinant ES1ADH. The relative activity of 100% means the full activity of recombinant and native enzymes (105 and 110 U mg⁻¹, respectively)

The conserved domain search of the deduced sequence indicated the regions (number of amino acid residues) from 22 to 372 and 22 to 400 were putative domains of iron-containing ADHs and class IV ADHs, respectively. In addition, the alignment of amino-terminal sequences from known ADHs from *Thermococcus* species indicated the presence of well-conserved residues, MxWESxx-xINQxFxxxxxT (Ma et al. 1994; Ma et al. 1995; Li and Stevenson 1997; Ronimus et al. 1997; Antoine et al. 1999). Sequence alignment of iron-containing ADHs from archaea and bacteria showed that 30 residues were strictly conserved, including conserved amino acid residues in putative iron-binding and coenzyme-binding sites (Fig. 1). The

monomer of ES1 ADH, like other proteins in the family, folded into two structural domains that were separated by a deep cleft (Fig. 2). The N-terminal domain (residues 1–182) was formed by an α/β region containing the dinucleotide-binding fold, whereas the C-terminal part (residues 183–383) was an all-helical domain.

Purification of native and recombinant ADHs

The ADH from *Thermococcus* strain ES1 was purified using three chromatography steps. A major separation was achieved using the DEAE-Sepharose column and the fractions with ADH activity showed only two dominant

bands after analysis by SDS-PAGE. The subsequent hydroxyapatite chromatography successfully separated the ADH from most contaminants (Fig. 3a). Gel filtration chromatography revealed that the size of the purified native enzyme was 182 ± 4 kDa. The purified ES1 ADH had a specific activity of 57 U mg^{-1} (assayed at pH 8.8) with a yield of 40% (Table 1). It was estimated that ADH represented about 10% of the protein in the cell-free extract and therefore was a highly abundant protein.

Table 2 Relative activities of native and recombinant ADHs towards alcohol oxidation

Alcohols (90 mM)	Native ES1ADH (%)	Recombinant ES1ADH (%)
Methanol	0	0
Ethanol	100 ± 2.6	91.6 ± 3.0
1-Propanol	120.6 ± 3.2	102.8 ± 2.0
1-Butanol	154.6 ± 5.2	142.6 ± 2.6
1-Pentanol	184 ± 3.2	175.6 ± 5.2
Hexyl alcohol	137.8 ± 4.0	114.4 ± 3.6
1-Heptanol	94 ± 3.6	100.8 ± 4.8
1-Octanol	68.8 ± 2.6	79 ± 1.0
2-Propanol	0	0
2-Butanol	0	0
2-Pentanol	0	0
2-Phenylethanol	40.2 ± 2.0	43 ± 1.5
Glycerol	0	0

Activities were determined using each substrate to replace 90 mM ethanol. The activity of native enzyme on ethanol ($110 \pm 2.9 \text{ U mg}^{-1}$) was taken as 100%

The recombinant ADH was purified from *E. coli* using a modified version of the procedure used to purify the native enzyme. For the recombinant ADH purification, a step was added in which the *E. coli* cell extract was incubated at 60°C for 1 h prior to chromatography. This caused no loss of ADH activity but significantly reduced the protein concentration from 13 to 2.9 mg ml^{-1} . Subsequently, the recombinant ADH was purified to homogeneity after DEAE-Sepharose column chromatography (Fig. 3b). The purified recombinant ES1 ADH had a specific activity of 52.8 U mg^{-1} (assayed at pH 8.8) with a yield of 75% (Table 1). The recombinant ES1ADH content in *E. coli* was calculated to be about 13% of the protein in the cell-free extract. Gel filtration analysis revealed that the recombinant enzyme was 176 ± 4 kDa in size, and SDS-PAGE analyses showed that both native and recombinant ES1ADHs had identical subunit sizes of 45 ± 1 kDa, suggesting that both enzymes were homotetramers in the native form (Fig. 3c). Moreover, the data from mass spectrometry indicated that the molecular mass of native and recombinant ES1ADH subunits were 44,819 and 44,831 Da, respectively, both of which were slightly greater than the theoretical molecular weight calculated from the deduced amino acid sequence of ES1ADH (44,807 Da).

Comparison of catalytic properties

The native and recombinant ADH enzymes had very similar catalytic properties. The effect of pH on enzyme activities was investigated with a set of buffers ranging from pH 5.5 to 11.0. The optimal pH for ethanol oxidation was pH 10.3–10.5 (Fig. 4a) and for acetaldehyde reduction

Table 3 Kinetic parameters of native and recombinant ES1ADHs

Substrate	Co-substrate (mM)	Parameter	Native	Recombinant
NADP ⁺	Ethanol (90)	Apparent K_m (mM)	0.06	0.058
		Apparent V_{\max} (U mg^{-1})	120	116
		k_{cat} (s^{-1})	90	87
		k_{cat}/K_m ($\text{s}^{-1} \text{ M}^{-1}$)	1,500,000	1,500,000
NADPH	Acetaldehyde (90)	Apparent K_m (mM)	0.007	0.006
		Apparent V_{\max} (U mg^{-1})	32	32
		k_{cat} (s^{-1})	24	24
		k_{cat}/K_m ($\text{s}^{-1} \text{ M}^{-1}$)	3,692,000	3,871,000
Ethanol	NADP ⁺ (0.4)	Apparent K_m (mM)	10.4	9.7
		Apparent V_{\max} (U mg^{-1})	112	108
		k_{cat} (s^{-1})	84	81
		k_{cat}/K_m ($\text{s}^{-1} \text{ M}^{-1}$)	8,000	8,000
Acetaldehyde	NADPH (0.4)	Apparent K_m (mM)	1.0	0.84
		Apparent V_{\max} (U mg^{-1})	31.4	30.5
		k_{cat} (s^{-1})	23.6	22.9
		k_{cat}/K_m ($\text{s}^{-1} \text{ M}^{-1}$)	24,000	27,000

was pH 7.0 (Fig. 4b). When the buffer pH values were higher than 10.5, the activity of ethanol oxidation had a remarkable decrease and no activity was detectable at pH 11.0. Over a temperature range from 30 to 95°C, the activity of both enzymes increased along with the increase of assay temperature (Fig. 5a), and they showed the same thermostability with determined $t_{1/2}$ -values at 95°C to be about 4 h (Fig. 5b).

Various primary and secondary alcohols were used in activity assays with NADP⁺ to investigate the substrate specificity of the two enzymes (Table 2). No activity with methanol, glycerol and secondary alcohols (2-propanol, 2-butanol and 2-pentanol) was detected. Primary alcohols with C₂–C₈ carbon chains provided 60–180% of the ADH activity compared with ethanol oxidation. Among C₂–C₈ primary alcohols, 1-pentanol gave the highest specific activity of 180 U mg⁻¹. In addition, ADH had 41 U mg⁻¹ of activity when 2-phenylethanol was the substrate.

The apparent K_m and V_{max} values for NADP⁺, ethanol, NADPH and acetaldehyde were determined (Table 3). The catalytic efficiency (k_{cat}/K_m) for NADPH and acetaldehyde was 2.5–3-fold greater than that for NADP⁺ and ethanol. Moreover, the K_m value of NADPH and acetaldehyde was almost 10 times lower than that of NADP⁺ and ethanol.

The metal content of the recombinant ADH was determined using ICP-MS. The results indicated the recombinant ADH contained 1 iron atom per subunit, which is consistent with the previous determination for the native enzyme (Ma et al. 1995). Although the recombinant ADH contained an additional 0.3 g zinc atom per subunit and trace amount of nickel (0.03 g atom per subunit), no inhibitory effect on the enzyme activity was observed. Similar to other known iron-containing ADHs, both recombinant and native forms of ES1 ADH were oxygen sensitive, and they lost almost 80% of their activity within 5 min exposure to the air. Their $t_{1/2}$ -values were estimated to be about 3 min (Fig. 5c). Unlike *T. hypogea* ADH, ES1ADH oxygen inactivation could not be protected by the presence of dithiothreitol (Ying et al. 2007).

Discussion

The production of recombinant versions of hyper/thermophilic proteins in mesophilic hosts such as *E. coli* is highly desirable due to simpler culture conditions, ease of purification using heat treatment, and typically higher yields. Although native ADH was present at a high concentration in the cells of *Thermococcus* strain ES1, recombinant *E. coli* had a much higher yield of ES1ADH (about 6 mg per gram cells) compared with *Thermococcus* strain ES1

(about 0.4 mg per gram cells). Moreover, the purification of ES1ADH from *E. coli* was greatly facilitated by a heat treatment step (Antoine et al. 1999).

The activity of recombinant ES1 ADH from *E. coli* did not require a heat activation step prior to assay. However, heat activation was essential to obtain maximally active forms of the iron-containing ADH from *T. hydrothermalis* and 2,3-butanediol ADH from *P. furiosus* (Antoine et al. 1999; Kube et al. 2006). The activity of the recombinant *T. hydrothermalis* ADH increased 10–25% after 1 min incubation at 80°C while *P. furiosus* ADH was inactive without heat treatment and the highest activity was obtained after a 10 min incubation at 100°C. Recombinant ES1 ADH activity was unaffected by heat-treating the cell-free extract, similar to what was observed with the recombinant short-chain ADH from *P. furiosus* (van der Oost et al. 2001). In addition, the catalytic and kinetic parameters of the native and recombinant enzymes were indistinguishable, indicating that this iron-containing ADH was successfully produced in *E. coli*. Furthermore, this study suggests that heterologous expression in *E. coli* could potentially be used for the large-scale production of this recombinant iron-containing hyperthermophilic ADH, as well as others from hyperthermophilic archaea, for potential biotechnological applications when catalysis can be carried out anaerobically.

ES1 ADH had biophysical and biochemical properties highly similar to characterized ADHs from other *Thermococcus* species (Table 4). The ADHs from *Thermococcus* species have a homotetrameric structure in the native form and are NADP⁺-dependent primary ADHs. Where data are available, the polypeptides for all *Thermococcus* ADHs contain 406 amino acids with an apparent molecular mass of 45 ± 1 kDa based on SDS-PAGE analysis. Sequence analyses indicated that ES1ADH is highly similar to iron-containing ADHs from *T. ethanolicus* (EAU56972) and *Clostridium cellulolyticum* (EAV69097) with identities of 69 and 64%, respectively. Compared to their mesophilic counterparts, the ratio of amino acid residues Arg, Gln, Pro and Tyr was increased by about a 1% molar fraction in hyper/thermophilic ADHs, whereas that of Ala, Asn and Val was decreased by about a 1% molar fraction (Gasteiger et al. 2005). The increased Gln content might well replace the decreased amount of Asn. However, it is very likely that other determinants are critical for thermostability, and detailed structural comparisons between the two types of enzyme are clearly necessary.

Both native and recombinant ES1ADHs were similarly oxygen-sensitive. The loss of activity after exposure to the air might be due to the oxidation of ferrous to ferric, and/or loss of ferrous ion, and replacement with other metals such as zinc (Ying et al. 2007). However, both enzymes could be successfully purified under anaerobic conditions,

Table 4 Comparison of ADHs from *Thermococcus* species

Organism	<i>Thermococcus</i> Stain ES1	<i>T. zilligii</i>	<i>T. hydrothermalis</i>	<i>T. litoralis</i>
Growth	91	75–80	85	85
T _{opt} (°C)				
Amino acids residues	406	406	406	ND
Size (kDa)	45	45	45	48 ^a
ADH content in cell (%, w/w) ^b	10	1.4	1.1	1.3
Type of ADH	Primary	Primary	Primary	Primary
Coenzyme	NADP(H)	NADP(H)	NADP(H)	NADP(H)
Reference	This study; Pledger and Baross (1989)	Klages and Morgan (1994); Li and Stevenson (1997); Ronimus et al. (1997)	Antoine et al. (1999)	Neuner et al. (1989); Ma et al. (1994)

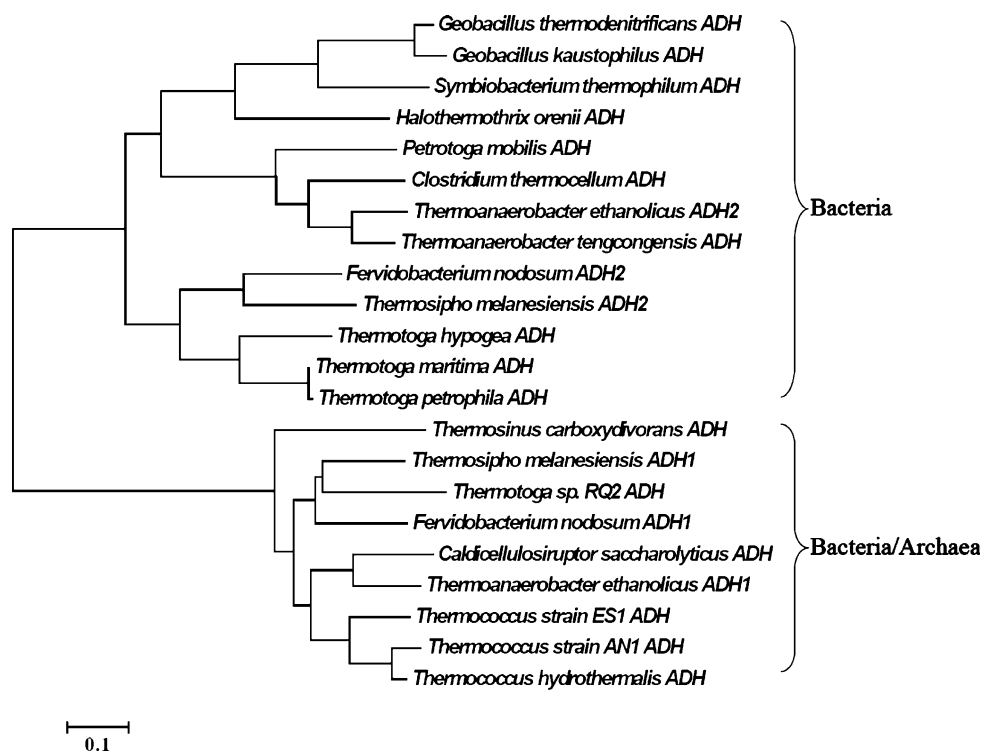
T_{opt}, optimal growth temperature^a Molecular mass estimated from SDS-PAGE^b Estimated values based on the amount of the ADH present in the cell-free extract

Fig. 6 Phylogenetic relationship between ES1 ADH and related iron-containing ADHs. The sequences were aligned using Clustal W and subsequently a phylogenetic tree was constructed by the neighbor-joining method (Thompson et al. 1994; Tamura et al. 2007). The scale bar represents 0.1 substitutions per sequence position. The accession numbers of ADH amino acid sequences used for the unrooted tree are as follows: *Geobacillus thermodenitrificans* NG80-2 (ABO68223); *G. kaustophilus* HTA426 (BAD77210); *Symbiobacterium thermophilum* IAM 14863 (BAD39520); *Haloferoxax orenii* H 168 (EAR79144); *Petrotoga mobilis* SJ95 (EDJ82753); *Clostridium thermocellum* ATCC

27405 (ABN51342); *Thermoanaerobacter ethanolicus* X514 (ADH1, EAU57309; ADH2, EAU57964); *T. tengcongensis* MB4 (AAM23605); *Fervidobacterium nodosum* Rt17-B1 (ADH1, EAV18253; ADH2, ABS61516); *T. melanesiensis* B1429 (ADH1, EAX34116; ADH2, ABR30668); *Thermotoga hypogaea* (Ying 2007); *T. maritima* (AAD35902); *T. petrophila* (ABQ46136); *Thermosinus carboxydvorans* Nor1 (EAX47257); *Thermotoga* sp. RQ2 (CAD67961); *Caldicellulosiruptor saccharolyticus* DSM 8903 (ABP66246); *Thermococcus* strain ES1 (EU919177); *Thermococcus* strain AN1 (AAB63011); *Thermococcus hydrothermalis* (CAA74334)

suggesting the ferrous ion was bound tightly enough for the purification. The irreversible loss of enzyme activity was also likely to be caused by the oxidation of some amino

acids such as cysteine residues resulting in irreversible structure change and thus inactivation of activity (Neale et al. 1986). A single amino acid residue is critical for the

aerobic inactivation of iron-containing ADHs in the facultative anaerobe *E. coli*. For example, propanediol oxidoreductase (FucO protein) in *E. coli* contains Fe and is sensitive to oxygen (Lu et al. 1998), and mutations near the NAD-binding consensus amino acid sequence (Ile7Leu and Leu8Val) increases resistance to oxidative stress at the cost of decreased thermal stability. Furthermore, the single substitution of Glu568Lys in AdhE, another iron-containing ADH in *E. coli*, yields functional enzyme under aerobic growth (Holland-Staley et al. 2000). It is not clear how the substitution Glu568Lys enables AdhE to be functional under aerobic culturing conditions. In contrast to *E. coli*, *Thermococcus* Strain ES1 is a strict anaerobe and is not exposed to oxygen in its natural ecosystem. Such a mechanism of aerobic inactivation as seen for the *E. coli* ADHs may not be involved. How oxygen alters the structure of Fe-containing ADHs is not well understood. Iron-sulfur centers are the oxidation-sensitive sites in several metalloproteins (Unden et al. 1994), but these are not present in ES1 ADH. A more oxygen tolerant form of ES1 ADH is highly desirable, and this is the focus of on-going studies. ICP-MS analyses of recombinant ES1 ADH showed the presence of 0.3 g atom zinc per subunit, but the recombinant enzyme had the same activity as the native one. This implied that zinc might have a non-specific binding site on the enzyme, which had no effect on the activity. Compared to the iron-containing ADH from *T. hypogea* (Ying et al. 2007), ES1 ADH seemed to be more resistant to exogenous zinc inhibition than the hyperthermophilic bacterial ADH.

The activity of ES1 ADH is regulated by the concentration of S^0 when *Thermococcus* Strain ES1 cells are grown on peptide-containing medium (Ma et al. 1995). The physiological role of ADH is proposed to be in the disposal of excess reductant under S^0 -limited conditions; however, the very high cellular content of the enzyme in the cell-free extract (up to 10% of cell protein) suggests that the enzyme has other physiological roles, and this aspect warrants further investigation.

The amino-terminal sequence of 19 amino acids (MxWESxxxINQxFxxxxxT) was highly conserved only in ADHs from *Thermococcus* species, which could be used as a unique molecular marker for identifying members of this class of ADH. Moreover, further analyses of primary structures showed that ES1ADH had structural similarity to other iron-containing ADHs from both hyperthermophiles and mesophiles. ES1 ADH had typical iron- and coenzyme-binding sites, Asp₂₀₉His₂₁₃His₂₇₈His₂₉₃ and Gly₁₁₀Gly₁₁₁Gly₁₁₂Ser₁₁₃X_{114–115}Asp₁₁₆, respectively. The structural modeling was based on the crystal structure of a putative iron-containing ADH from *T. maritima* (TM0820) as the 3-D structure of an ADH from a hyperthermophilic archaeon is not available. The structural modeling clearly

showed two typical domains belonging to the family of iron-containing ADHs, the α/β -dinucleotide-binding N-terminal domain and the all- α -helix C-terminal domain separated by a deep cleft (Schwarzenbacher et al. 2004; Montella et al. 2005). However, an experimentally determined three-dimensional structure is required to confirm the structural modeling prediction. Based on sequence similarity, iron-containing ADHs from hyper/thermophiles could be divided into two groups, one that is only present in the *Bacteria* domain, and another that is present in both domains of *Bacteria* and *Archaea* (Fig. 6). The ES1ADH belonged to the latter group. It is an open question as to what extent the divergent evolution of these enzymes reflects their physiological functions, which are generally unknown at present.

Acknowledgments This work was supported by research grants from Natural Sciences and Engineering Research Council (Canada), Ontario Ministry of Agriculture and Food—Rural Affairs and Canada Foundation for Innovation to KM, and by a grant (BES-061723) from the US National Science Foundation to MA.

References

- Altschul SF, Madden TL, Schäffer AA, Zhang J, Zhang Z, Miller W, Lipman DJ (1997) Gapped BLAST and PSI-BLAST: a new generation of protein database search programs. *Nucleic Acids Res* 25:3389–3402
- Antoine E, Rolland JL, Raffin JP, Dietrich J (1999) Cloning and overexpression in *Escherichia coli* of the gene encoding NADPH group III alcohol dehydrogenase from *Thermococcus hydrothermalis*. *Eur J Biochem* 264:880–889
- Bateman A, Birney E, Cerruti L, Durbin R, Ewiler L, Eddy SR, Griffiths-Jones S, Howe KL, Marshall M, Sonnhammer EL (2002) The Pfam protein families database. *Nucleic Acids Res* 30:276–280
- Bradford MM (1976) A rapid and sensitive method for the quantitation of microgram quantities of protein utilizing the principle of protein-dye binding. *Anal Biochem* 72:248–254
- Cannio R, Fiorentino G, Carpinelli P, Rossi M, Bartolucci S (1996) Cloning and overexpression in *Escherichia coli* of the genes encoding NAD-dependent alcohol dehydrogenase from two *Sulfolobus* species. *J Bacteriol* 178:301–305
- Conway T, Ingram LO (1989) Similarity of *Escherichia coli* propanediol oxidoreductase (fucO product) and an unusual alcohol dehydrogenase from *Zymomonas mobilis* and *Saccharomyces cerevisiae*. *J Bacteriol* 171:3754–3759
- Delano WL (2002) The PyMOL molecular graphics system. Delano Scientific, Palo Alto
- Gasteiger E, Hoogland C, Gattiker A, Duvaud S, Wilkins MR, Appel RD, Bairoch A (2005) Protein identification and analysis tools on the ExPASy Server. In: Walker JM (ed) *The proteomics protocols handbook*. Humana Press, Totowa, pp 571–607
- Guex N, Peitsch MC (1997) SWISS-MODEL and the Swiss-PdbViewer: an environment for comparative protein modelling. *Electrophoresis* 18:2714–2723
- Hirakawa H, Kamiya N, Kawarabayashi Y, Nagamune T (2004) Properties of an alcohol dehydrogenase from the hyperthermophilic archaeon *Aeropyrum pernix* K1. *J Biosci Bioeng* 97:202–206

- Holland-Staley CA, Lee K, Clark DP, Cunningham PR (2000) Aerobic activity of *Escherichia coli* alcohol dehydrogenase is determined by a single amino acid. *J Bacteriol* 182:6049–6054
- Hummel W (1999) Large-scale applications of NAD(P)-dependent oxidoreductases: recent developments. *Trends Biotechnol* 17:487–492
- Klages KU, Morgan HW (1994) Characterization of an extremely thermophilic sulphur-metabolizing archaeobacterium belonging to the *Thermococcales*. *Arch Microbiol* 162:261–266
- Kopp J, Schwede T (2004) The SWISS-MODEL repository of annotated three-dimensional protein structure homology models. *Nucleic Acids Res* 32:D230–D234
- Kube J, Brokamp C, Machielsen R, van der Oost J, Märkl H (2006) Influence of temperature on the production of an archaeal thermoactive alcohol dehydrogenase from *Pyrococcus furiosus* with recombinant *Escherichia coli*. *Extremophiles* 10:221–227
- Laemmli UK (1970) Cleavage of structural proteins during assembly of the head of bacteriophage T4. *Nature* 227:680–685
- Leary JJ, Brigati DJ, Ward DC (1983) Rapid and sensitive colorimetric method for visualization of biotin-labeled DNA probes hybridized to DNA or RNA immobilized on nitrocellulose: bioblots. *Proc Natl Acad Sci USA* 80:4045–4049
- Li D, Stevenson KJ (1997) Purification and sequence analysis of a novel NADP(H)-dependent type III alcohol dehydrogenase from *Thermococcus* strain AN1. *J Bacteriol* 179:4433–4437
- Lu Z, Cabisco E, Obradors N, Tamarit J, Ros J, Aguilar J, Lin ECC (1998) Evolution of an *Escherichia coli* protein with increased resistance to oxidative stress. *J Biol Chem* 273:8308–8316
- Ma K, Adams MWW (1999) An unusual oxygen-sensitive, iron- and zinc-containing alcohol dehydrogenase from the hyperthermophilic archaeon, *Pyrococcus furiosus*. *J Bacteriol* 181:1163–1170
- Ma K, Adams MWW (2001) Alcohol dehydrogenases from *Thermococcus litoralis* and *Thermococcus* strain ES-1. *Meth Enzymol* 331:195–201
- Ma K, Loessner H, Heider J, Johnson MK, Adams MWW (1995) Effects of elemental sulfur on the metabolism of the deep-sea hyperthermophilic archaeon *Thermococcus* strain ES-1: characterization of a sulfur-regulated, non-heme iron alcohol dehydrogenase. *J Bacteriol* 177:4748–4756
- Ma K, Robb FT, Adams MWW (1994) Purification and characterization of NADP-specific alcohol dehydrogenase and glutamate dehydrogenase from the hyperthermophilic archaeon *Thermococcus litoralis*. *Appl Environ Microbiol* 60:562–568
- Machielsen R, Uria AR, Kengen SWM, van der Oost J (2006) Production and characterization of a thermostable alcohol dehydrogenase that belongs to the aldo-keto reductase superfamily. *Appl Environ Microbiol* 72:233–238
- Montella C, Bellolell L, Pérez-Luque R, Badía J, Baldoma L, Coll M, Aguilar J (2005) Crystal structure of an iron-dependent group III dehydrogenase that interconverts L-lactaldehyde and L-1,2-propanediol in *Escherichia coli*. *J Bacteriol* 187:4957–4966
- Neale AD, Scopes RK, Kelly JM, Wettenhall RE (1986) The two alcohol dehydrogenases of *Zymomonas mobilis*. Purification by differential dye ligand chromatography, molecular characterisation and physiological roles. *Eur J Biochem* 154:119–124
- Neuner A, Jannasch HW, Belkin S, Stetter KO (1989) *Thermococcus litoralis* sp. nov.: a new species of extremely thermophilic marine archaeobacteria. *Arch Microbiol* 153:205–207
- Peitsch MC (1995) Protein modeling by E-mail. *Bio Technol* 13:658–660
- Pledger RJ, Baross J (1989) Characterization of an extremely thermophilic archaeobacterium isolated from a black smoker polychaete (*Paralvinella*, sp.) at the Juan de Fuca Ridge. *Syst Appl Microbiol* 12:249–256
- Reid MF, Fewson CA (1994) Molecular characterization of microbial alcohol dehydrogenases. *Crit Rev Microbiol* 20:13–56
- Ronimus RS, Reysenbach AL, Musgrave DR, Morgan HW (1997) The phylogenetic position of the *Thermococcus* isolate AN1 based on 16S rRNA gene sequence analysis: a proposal that AN1 represents a new species, *Thermococcus zilligii* sp. nov. *Arch Microbiol* 168:245–248
- Sambrook J, Russell DW (2001) Molecular cloning: a laboratory manual. Cold Spring Harbor Laboratory Press, Cold Spring Harbor
- Schwarzenbacher R, von Delft F, Canaves JM, Brinen LS, Dai X, Deacon AM, Elsliger MA, Eshaghi S, Floyd R, Godzik A, Grittini C, Grzechnik SK, Guba C, Jaroszewski L, Karlak C, Klock HE, Koesema E, Kovarik JE, Kreusch A, Kuhn P, Lesley SA, McMullan D, McPhillips TM, Miller MA, Miller MD, Morse A, Moy K, Ouyang J, Page R, Robb A, Rodrigues K, Selby TL, Spraggon G, Stevens RC, van den Bedem H, Velasquez J, Vincent J, Wang X, West B, Wolf G, Hodgson KO, Wooley J, Wilson IA (2004) Crystal structure of an iron-containing 1,3-propanediol dehydrogenase (TM0920) from *Thermotoga maritima* at 1.3 Å resolution. *Proteins* 54:174–177
- Schwede T, Kopp J, Guex N, Peitsch MC (2003) SWISS-MODEL: an automated protein homology-modeling server. *Nucleic Acids Res* 31:3381–3385
- Stetter KO (1988) Hyperthermophiles—physiology and enzymes. *J Chem Technol Biotechnol* 42:315–317
- Tamura K, Dudley J, Nei M, Kumar S (2007) *MEGA4*: molecular evolutionary genetics analysis (MEGA) software version 4.0. *Mol Biol Evol* 24:1596–1599
- Thompson JD, Higgins DG, Gibson TJ (1994) CLUSTAL W: improving the sensitivity of progressive multiple sequence alignment through sequence weighting, position-specific gap penalties and weight matrix choice. *Nucleic Acids Res* 22:4673–4680
- Uden G, Becker S, Bongaerts J, Schirawski J, Six S (1994) Oxygen regulated gene expression in facultatively anaerobic bacteria. *Antonie Leeuwenhoek* 66:3–23
- van der Oost J, Voorhorst WGB, Kengen SWM, Geerling ACM, Wittenhorst V, Gueguen Y, de Vos WM (2001) Genetic and biochemical characterization of a short-chain alcohol dehydrogenase from the hyperthermophilic archaeon *Pyrococcus furiosus*. *Eur J Biochem* 268:3062–3068
- Walter KA, Bennett GN, Papoutsakis ET (1992) Molecular characterization of two *Clostridium acetobutylicum* ATCC 824 butanol dehydrogenase isozyme genes. *J Bacteriol* 174:7149–7158
- Ying X (2007) Characterization of iron- and zinc-containing alcohol dehydrogenases from anaerobic hyperthermophiles. PhD Thesis, University of Waterloo, Waterloo, Canada. <http://hdl.handle.net/10012/3446>
- Ying X, Wang Y, Badiei HR, Karanassios V, Ma K (2007) Purification and characterization of an iron-containing alcohol dehydrogenase in extremely thermophilic bacterium *Thermotoga hypogea*. *Arch Microbiol* 187:499–510
- Zheng Y, Cao Y, Fang B (2004) Cloning and sequence analysis of the *dhaT* gene of the 1,3-propanediol regulon from *Klebsiella pneumoniae*. *Biotechnol Lett* 26:251–255